Comparison of sound reproduction using higher order loudspeakers and equivalent line arrays in free-field conditions

Mark A. Poletti[a] and Terence Betlehem
Callaghan Innovation, P.O. Box 31-310, Lower Hutt, New Zealand

Thushara D. Abhayapala
Research School of Engineering, Australia National University College of Engineering and Computer Science, The Australian National University, Canberra, Australia

Higher order sound sources of Nth order can radiate sound with $2N+1$ orthogonal radiation patterns, which can be represented as phase modes or, equivalently, amplitude modes. This paper shows that each phase mode response produces a spiral wave front with a different spiral rate, and therefore a different direction of arrival of sound. Hence, for a given receiver position a higher order source is equivalent to a linear array of $2N+1$ monopole sources. This interpretation suggests performance similar to a circular array of higher order sources can be produced by an array of sources, each of which consists of a line array having monopoles at the apparent source locations of the corresponding phase modes. Simulations of higher order arrays and arrays of equivalent line sources are presented. It is shown that the interior fields produced by the two arrays are essentially the same, but that the exterior fields differ because the higher order sources produces different equivalent source locations for field positions outside the array. This work provides an explanation of the fact that an array of L Nth order sources can reproduce sound fields whose accuracy approaches the performance of $(2N+1)L$ monopoles. © *2014 Acoustical Society of America*. [http://dx.doi.org/10.1121/1.4883363]

I. INTRODUCTION

Recently it has been shown that loudspeakers which can radiate sound with multiple radiation patterns, known as higher-order (HO) loudspeakers, can produce improved sound reproduction over monopole loudspeakers.[1,2] While higher-order loudspeakers require the use of multiple drivers, a small number of HO units is more convenient and easier to position in a room than a large number of single-driver (or woofer-tweeter) loudspeakers.

A 2D higher-order loudspeaker of order N produces $2N+1$ modes of sound radiation with azimuthal phase mode responses of the form $\exp(in\phi)$ or, equivalently, amplitude mode responses of the form $\cos(n\phi)$ and $\sin(n\phi)$ for integers n and angle ϕ.[3,4] A circular array of Nth-order loudspeakers can reproduce sound accurately up to the spatial Nyquist frequency of the array (defined as the frequency where reproduction of a sound field is accurate throughout the interior of the array), and this value approaches $2N+1$ times the spatial Nyquist frequency of an equal number of monopole loudspeakers. This claim was verified by simulations in Ref. 2.

If higher-order loudspeakers are used in a semi-reverberant room, then calibration using a higher-order microphone may be used to compensate for the effects of reverberation. In this case the loudspeakers can direct sound from the room surfaces and achieve better reproduction than

would be produced in the free-field case.[5,6] The reflections from the wall surfaces provided more direction of arrival of sound, increasing the diversity of the reproduction environment.

A limitation of higher order loudspeakers in the free-field case is that they cannot provide an improvement in sound reproduction accuracy if the loudspeakers are at large distances from the listener. This is easily seen because for large distances, the sound fields produced at the origin by an array of higher order loudspeakers are planar and cannot produce results which are different from an array of monopole loudspeakers at the same distance. In practice, of course, the loudspeakers are always relatively close to the listener and the $2N+1$ improvement can be approximated, particularly when in a semi-reverberant room. However, the accuracy of reproduction in the free-field case will depend on the distance to the loudspeakers.

This paper undertakes a more detailed investigation of the behavior of higher order loudspeakers, in order to better understand the mechanism by which they produce an increase in reproduction accuracy. It is shown that each phase mode of the higher order loudspeaker produces wave fronts which form a spiral. Transducers producing first order spiral fields have been recently developed for use in underwater bearing estimation.[7–9] This idea is extended to the general case and it is shown that for a given position in space, each spiral wave front appears to come from a different source position. Hence, for free-field reproduction within a circular array of higher order sources each Nth order speaker is similar in performance to an array of $2N+1$ point sources,

[a] Author to whom correspondence should be addressed. Electronic mail: mark.poletti@callaghaninnovation.govt.nz

with positions governed by the wave front curvature of each higher order phase mode.

For simplicity the 2D case is considered, as in previous work. However the properties of a 3D spherical higher order source are also considered and it is shown that, in the case of 2D reproduction in a plane, the phase mode properties of 3D sources are the same as for 2D sources. The investigation is restricted to the creation of interior sound fields without attempting to cancel the exterior field. In this paper a time dependency of $\exp(i\omega t)$ is assumed.

II. EQUIVALENT SOURCE DESCRIPTION OF HIGHER ORDER LOUDSPEAKERS

It is now shown that the higher order modes produce an equivalent monopole source at a position defined by the wavelength and the mode order.

A. 2D higher order sources

The solution to the wave equation in polar coordinates (r, ϕ) for a region $r > r_0$ exterior to any sound sources is[10]

$$p_E(r, \phi, k) = \sum_{n=-\infty}^{\infty} H_n(kr) B_n(k) e^{in\phi}, \qquad (1)$$

where $B_n(k)$ is the nth exterior sound field expansion coefficient, $H_n(x) = H_n^{(2)}(x)$ is the nth order Hankel function of the second kind, $k = \omega/c$ is the wave number, and c is the speed of sound.

Consider a source at the origin, of radius R, with a radial velocity which can be written

$$v_r(\phi) = V_0 \sum_{n=-N}^{N} \alpha_n e^{in\phi}, \qquad (2)$$

where N is the order of the expansion and α_n is the Fourier series coefficient of the nth term. By requiring that the radial velocity of the general expression in Eq. (1) equals the surface velocity Eq. (2) at $r = R$, it can be shown that the 2D exterior field has the form[1]

$$p_E(r, \phi, k) = i\rho c V_0 \sum_{n=-N}^{N} \alpha_n \frac{H_n(kr)}{H'_n(kR)} e^{in\phi}. \qquad (3)$$

The sound field is a sum of $2N + 1$ terms, and the sound source is referred to as an Nth order source. Each term is known as a phase mode,[3] and its frequency-dependent amplitude and phase are governed by the Hankel function $H_n(kr)$ and the Hankel function derivative $H'_n(kR)$. Since each mode can be independently controlled, the source can be equalized in such a way to produce frequency-independent polar responses over a finite frequency range.[1]

B. Equivalent source position of a phase mode

The nth term in Eq. (3) has the general form

$$p_{E,n}(r, \phi, k) = \beta_n \frac{H_n(kr)}{H'_n(kR)} e^{in\phi}, \quad r > R, \qquad (4)$$

where β_n is a constant. The Hankel function has the form[11]

$$H_n(kr) = \sqrt{\frac{2}{\pi kr}} i^{n+1/2} e^{-ikr}$$
$$\times \left[\sum_{q=0}^{p-1} \frac{1}{q!} \frac{\Gamma(n+q+1/2)}{\Gamma(n-q+1/2)} \left(\frac{-i}{2kr} \right)^q + O(z^{-p}) \right], \qquad (5)$$

where $O(z^{-p})$ has a magnitude of order z^{-p} as z tends to infinity.

For $2kr \gg 1$ this can be approximated as

$$H_n(kr) \approx \sqrt{\frac{2}{\pi kr}} i^{n+1/2} e^{-ikr}. \qquad (6)$$

The derivative of the Hankel function, $H'_n(kR)$, governs the response of the nth phase mode with frequency. It does not vary with radius r and so is a constant complex number for a given wave number k and source radius R. In typical applications the nth mode response would be equalized, and therefore the phase of $H'_n(kR)$ may be ignored. The constant $i^{n+1/2}$ may also be ignored, by the same argument.

The sound field of the nth phase mode is therefore, for distances $r \gg 1/(2k)$, of the general form

$$p_{E,n}(r, \phi, k) = \gamma_n e^{i(n\phi - kr)}, \quad r > R, \qquad (7)$$

where γ_n is a constant, and the phase of the nth mode field varies with radius r and azimuth ϕ, as

$$\Phi_n(r, \phi) = n\phi - kr. \qquad (8)$$

The phase is zero for $r = n\phi/k$, which is the definition of an Archimedes spiral.[12] Hence the wave front where the phase is zero is of the form of an Archimedes spiral. More precisely, the spatial component of the sound field produced by the nth phase mode has n loci along which the phase is zero. These are given by the condition $n\phi - kr + l2\pi = 0$ for $l \in [0, n-1]$ and define Archimedes spirals $\vec{r}_l(\phi) = (x_l(\phi), y_l(\phi))$ with x and y coordinates

$$x_l(\phi) = \frac{n\phi}{k} \cos\left(\phi + \frac{l2\pi}{n} \right), \qquad (9)$$

$$y_l(\phi) = \frac{n\phi}{k} \sin\left(\phi + \frac{l2\pi}{n} \right). \qquad (10)$$

The gradient of the curve with respect to ϕ is the tangent to the wave front, $\vec{\tau}_l = (x'_l(\phi), y'_l(\phi))$, and the normal, $\vec{\eta}_l(\phi) = (-y'_l(\phi), x'_l(\phi))$, is then the negative of the direction of propagation, with components

$$\eta_{xl}(\phi) = -\frac{n}{k}(\phi \cos(\phi + l2\pi/n) + \sin(\phi + l2\pi/n)), \quad (11)$$

$$\eta_{yl}(\phi) = \frac{n}{k}(\cos(\phi + l2\pi/n) - \phi \sin(\phi + l2\pi/n)). \quad (12)$$

For a given field position (x, y), the normal to the wave front points towards the source position of a monopole which

J. Acoust. Soc. Am., Vol. 136, No. 1, July 2014

Poletti *et al.*: Higher order loudspeaker and line array   193

would produce the same wave front. For simplicity a point on the x axis is assumed. The normal vector at zero phase on the x axis, for positive x values, occurs for $\phi + l2\pi/n = v2\pi$, for integers v. The normal is, for these cases,

$$\vec{\eta}(x) = \left(-x, \frac{n}{k}\right). \tag{13}$$

Hence, for positive x values the wave fronts from the nth mode appear to originate from a point on the y axis equal to

$$y_n = \frac{n}{k}. \tag{14}$$

Note that the distance relative to the wavelength, λ, is a constant,

$$\frac{y_n}{\lambda} = \frac{n}{2\pi}. \tag{15}$$

The corresponding angle of the nth source from the x axis is

$$\alpha_n = \tan^{-1}\left(\frac{n}{kx}\right). \tag{16}$$

In general, for a field position at angle ϕ_0 the equivalent source position is

$$
\begin{aligned}
&(x_n(\phi_0), y_n(\phi_0)) \\
&= \left(-\frac{n}{k}\cos(\phi_0 + \pi/2), \frac{n}{k}\sin(\phi_0 + \pi/2)\right),
\end{aligned} \tag{17}
$$

which is rotated $90°$ from the field angle and is at a distance n/k from the center of the source. This behavior is shown in Figs. 1 and 2, where the real part of the first and second order modes for a source of radius $R = 0.25$ m are shown. Figure 1 shows the field due to a first order source. The normals to the spiral wave fronts are drawn for three values of x. The equivalent source distance from the origin is $y_n = 0.108$ m, shown as a circle in Fig. 1. The normals all converge on the
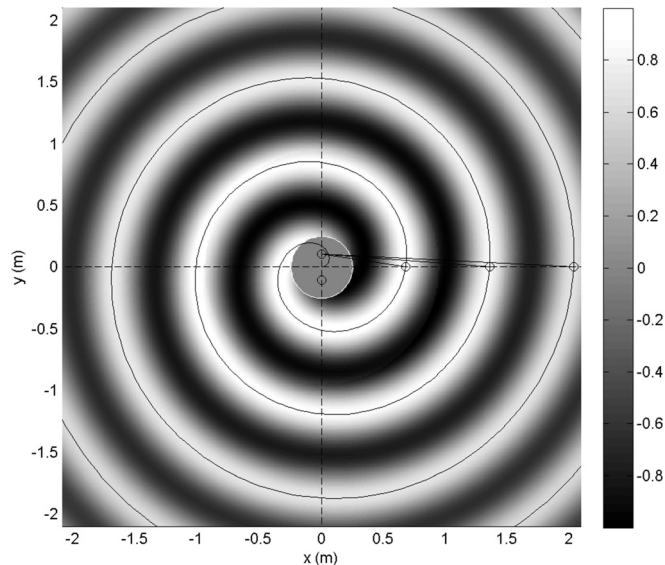

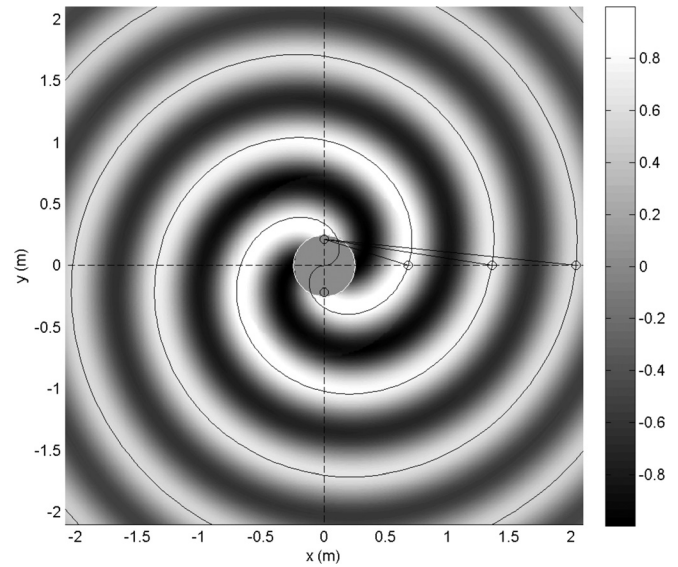FIG. 1. Sound field for $R = 0.25$, $n = 1$ at 500 Hz, $y_1 = 0.1$ m.

equivalent source position. The equivalent source positions for sources on the negative x axis are at $y_n = -0.108$ m, showing that the equivalent source position depends on the field position.

Figure 2 shows the field for a second order source. The apparent source distance is a larger value of $y_n = 0.216$ m, slightly less than the source radius R. The three normals again converge on the equivalent source position.

Equation (14) suggests that at low frequencies the source position distances from the center of the loudspeaker are greater than the radius R. While this is true, the magnitudes of the source is given by the magnitude of Eq. (4). These are shown in Fig. 3.[1] The magnitudes roll-off below the "activation" frequency given by $kR = n$, or

$$f_n = \frac{nc}{2\pi R}, \tag{18}$$

shown as circles in Fig. 3. Since $n = kR$ defines the activation frequency, and $n = y_n k$ defines the lateral source position, the nth source distance y_n equals the loudspeaker radius at the mode activation frequency. For frequencies lower than f_n, the source distance is greater than R, but the magnitude of the response rapidly reduces, particularly for higher orders. Hence, it is not physically possible to position a source at large distances from the loudspeaker that also produces significant sound pressure. The mode activation frequency was 217 Hz in Fig. 1 and the equivalent monopole source position is $y = 0.1$ m, nearly half the speaker radius. In Fig. 2 the activation frequency is 433 Hz which is close to the source frequency, and the source position is 0.22 m, near the edge of the loudspeaker.

Applying the analysis above to a surround sound system, it can be said that a higher order loudspeaker at a distance r_L from the origin, and at angle ϕ_l, producing $2N+1$ modes, behaves as a line array of $2N+1$ monopole sources at radii r_L with distances from the speaker center, tangent to the speaker radius, given by
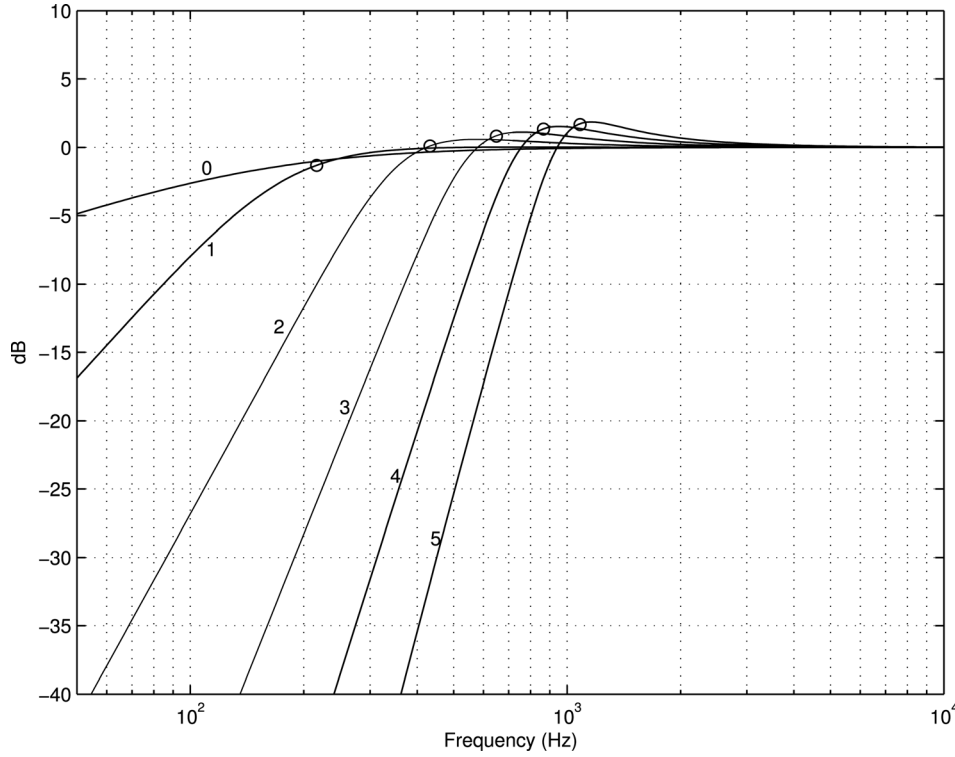

FIG. 2. Sound field for $R = 0.25$ m, $n = 2$ at 500 Hz, $y_2 = 0.22$ m.

FIG. 3. Mode responses for $R = 0.25$ m. Activation frequencies shown as circles.

$$y_n = \frac{n}{k}, \quad n \in [-N, N] \tag{19}$$

and source angles given by

$$\phi_{l,n} = \phi_l + \tan^{-1}\left(\frac{n}{kr_L}\right), \quad n \in [-N : N], \tag{20}$$

where the magnitudes of each source reduce for distances greater than the source radius, i.e., below the corresponding activation frequency.

C. 3D higher order sources

It will now be shown that 3D higher order sources display the same equivalent monopole source positions as 2D sources.

The solution to the wave equation in spherical coordinates (r, θ, ϕ) for a region $r > r_0$ exterior to any sound sources is[10]

$$p_E(r, \theta, \phi, k) = \sum_{n=0}^{\infty} \sum_{m=-n}^{n} B_n^m(k) h_n(kr) Y_n^m(\theta, \phi), \tag{21}$$

where $h_n(x)$ is the spherical Hankel function of the second kind,[10] and the spherical harmonics are defined as[13]

$$Y_n^m(\theta, \phi) = \sqrt{\frac{(2n+1)}{4\pi}\frac{(n-|m|)!}{(n+|m|)!}}P_n^{|m|}(\cos\theta)e^{im\phi}, \tag{22}$$

where $P_n^m(\cdot)$ is the associated Legendre function.[10]

Consider a sphere of radius R vibrating with surface velocity

$$v(\theta_s, \phi_s, t) = e^{i\omega t}\sum_{n=0}^{\infty}\sum_{m=-n}^{n}\alpha_n^m Y_n^m(\theta_s, \phi_s). \tag{23}$$

Following the same procedure as for the 2D case, it may be shown that the exterior field has the general form[14–18]

$$p_E(r, \theta, \phi) = i\rho c\sum_{n=0}^{\infty}\sum_{m=-n}^{n}\frac{\alpha_n^m}{h'_n(ka)}h_n(kr)Y_n^m(\theta, \phi), \quad r \geq a. \tag{24}$$

The (n,m)th mode then has the form

$$p_{E,n,m}(r, \theta, \phi) = \gamma_n^m\frac{h_n(kr)}{h'_n(kR)}Y_n^m(\theta, \phi), \quad r \geq r_0, \tag{25}$$

where γ_n^m is a constant. The spherical Hankel function has the form[11]

$$h_n(kr) = \frac{i^{n+1}e^{-ikr}}{kr}\sum_{q=0}^{n}\frac{1}{q!}\frac{(n+q)!}{(n-q)!}\left(\frac{-i}{2kr}\right)^q. \tag{26}$$

For $2kr \gg 1$ the sound pressure is approximated by

$$p_{E,n,m}(r, \theta, \phi) = \gamma_n^m i^{n+1}\frac{Y_n^m(\theta, 0)}{kh'_n(kR)}\frac{e^{-ikr}}{r}e^{im\phi}, \quad r \geq r_0. \tag{27}$$

Hence, as for the 2D case, the constant phase may be ignored, and the sound field for a given θ produces loci of constant phase which are Archimedes spirals.

In the 2D case, where the reproduced field is in the (x,y) plane, and for the sectorial modes where $n = |m|$, the responses in elevation are of the form $(\sin\theta)^{|m|}$, which produce a single lobe at $\theta = \pi/2$, in the (x,y) plane. In this case the equivalent source position seen at a position in the (x,y) plane is given by Eq. (17). However, for field positions at other values of θ the amplitude of the source reduces, suggesting that the equivalent source must have a non-zero

aperture in z. For non-sectorial modes, the response in elevation is more complex with peaks and nulls governed by the associated Legendre function $P_n^{|m|}(\cos\theta)$. Such responses can be produced by a line array of monopoles with suitable weightings.

In summary, for reproduction in the (x,y) plane the equivalent monopole source position is the same as for the 2D case, but in general a monopole array in z, positioned in the (x,y) plane according to Eq. (17), and implementing a polar response in elevation equal to an associated Legendre function, provides a more accurate description.

In general, the spherical harmonic description of a source is equivalent to a multipole expansion.[10] The model described here is an alternative that is simpler for modeling reproduction in the 2D case, and which produces a different equivalent source position for each field position.

III. COMPARISON OF HIGHER ORDER SOURCES WITH EQUIVALENT LINE ARRAYS

The previous section has shown that for 2D reproduction, an Nth order source is equivalent to $2N+1$ monopole sources with frequency-dependent source positions and magnitudes. Therefore a circular array of higher order sources is similar to a circular array of line arrays of $2N+1$ sources. Along the radial line from the origin to each higher order source, the corresponding equivalent monopole sources appear to be positioned tangential to the circle and centered at the higher order source position. Therefore, in free-field conditions, and for field positions that are not too close to the loudspeakers, the sound reproduction performance of an array of L higher order sources should be similar to that of a circular array of L sources, each consisting of a line array of $2N+1$ monopoles. However, since the position of the equivalent monopoles varies with field position, the sound fields produced by the two arrays will differ for field positions close to the loudspeakers. Furthermore, for positions exterior to the array, the positions of the sources for higher order speakers close to the field position will be reversed, while those from the far side of the array will have the same positions. Hence, the exterior field produced by a higher order array will differ from that of a fixed array of line arrays.

To investigate this, numerical simulations of 2D sound reproduction using both higher order sources and line arrays of monopoles are carried out. A brief outline of the method for determining the higher order source weightings is given here. Further details are given in Ref. 1.

A. Array of higher order sources

The desired sound field is a 2D interior sound field which has the general expansion[10]

$$p_I(r,\phi,k) = \sum_{m=-\infty}^{\infty} J_m(kr)A_m(k)e^{im\phi}, \qquad (28)$$

where $J_m(\cdot)$ is the mth cylindrical Bessel function and $A_m(k)$ is the mth sound field expansion coefficient. The expansion may be limited to order

$$M = \frac{ekr}{2}, \qquad (29)$$

where $e = \exp(1) = 2.718$, for a given k and r.[19,20]

The interior field is approximated using L Nth order sources at radius r_L and positioned at equally spaced angles $\phi_l = l2\pi/L$, $l \in [0, L-1]$. The interior sound field, for $r < r_L$, due to the nth mode of radiation of the lth higher order source is represented using the cylindrical addition theorem[11]

$$p_{n,l}(r,\phi,r_L\phi_l,k) = H_n(kr_0)e^{in\chi_l}$$
$$= \sum_{m=-\infty}^{\infty} J_m(kr)H_{m+n}(kr_L)e^{im(\phi-\phi_l)}, \qquad (30)$$

where the angle χ_l is defined in Fig. 4. The sum of all $L(2N+1)$ fields of the form of Eq. (4), weighted by complex amplitudes $w_{n,l}$, then has the form

$$\hat{p}_I(r,\phi,k) = \sum_{m=-\infty}^{\infty} J_m(kr)e^{im\phi}$$
$$\times \left[\sum_{l=1}^{L} \sum_{n=-N}^{N} w_{n,l} \frac{H_{m+n}(kr_L)}{H'_n(kR)} e^{-im\phi_l} \right], \quad r < r_L. \qquad (31)$$

Equating this approximated field to Eq. (28) produces the mode matching equations

$$\sum_{n=-N}^{N} \frac{H_{n+m}(kr_L)}{H'_n(kR)} \sum_{l=1}^{L} w_{n,l}e^{-im\phi_l} = A_m, \quad m \in [-M,M]. \qquad (32)$$

This equation may be written in matrix form

$$\mathbf{H}w = a, \qquad (33)$$

where $\mathbf{H}$ is a $2M+1$ by $(2N+1)L$ matrix, w is a $(2N+1)L$ by one vector of weights, and a is a $2M+1$ vector of interior coefficients.
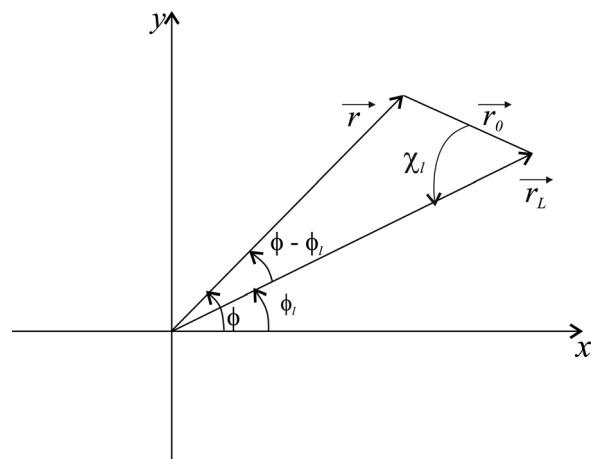

FIG. 4. Geometry for addition theorem.

It has been shown that solutions to Eq. (32) are more robust if the number of modes is limited so that $2M + 1 \leq L(2N + 1)$. Setting $2M + 1 = \psi L(2N + 1)$ where $\psi < 1$, and using Eq. (29) with $r = r_L$, the approximate spatial Nyquist frequency of the array is found to be[1]

$$f_N = \frac{c(\psi L(2N + 1) - 1)}{e 2 \pi r_L}. \tag{34}$$

The weights may then be determined from Eq. (33) as

$$w = \mathbf{H}^H [\mathbf{H}\mathbf{H}^H + \sigma \mathbf{I}]^{-1} a, \tag{35}$$

where $\mathbf{I}$ is the $2M + 1$ by $2M + 1$ identity matrix. For $\sigma = 0$ this is the minimum energy solution and σ can be used to reduce the weight solutions for cases where $\mathbf{H}$ has small singular values. In the simulations to be presented below, σ was set to a fraction $\varepsilon = 1e - 4$ of the squared maximum singular value of $\mathbf{H}$.

B. Array of line arrays

Each higher order source at angle ϕ_l is equivalent to $2N + 1$ monopoles at angles given by Eq. (20). A circular array of $L(2N + 1)$ monopoles with each array of $2N + 1$ monopoles centered at ϕ_l and with the monopole angles given by Eq. (20) is therefore equivalent to the higher order source array. It will be assumed, for simplicity, that all monopoles are at the radius r_L, so that each line array has a small amount of curvature. The sound field produced by each monopole source has the form of Eq. (4) with $n = 0$.

For correct reproduction the sound field produced by the sum of the fields produced by all $L(2N + 1)$ monopoles, weighted by complex amplitudes $q_{n,l}$ must equal Eq. (28). Each monopole sound field is given by Eq. (4) for $n = 0$ and $\beta_0 = 1$ and can be expressed at an arbitrary source position using the cylindrical addition theorem.[11] The resulting mode matching equations are

$$\frac{H_m(kr_L)}{H'_0(kR)} \sum_{n=-N}^{N} \sum_{l=1}^{L} q_{n,l} e^{-im\phi_{l,n}} = A_m, \quad m \in [-M, M]. \tag{36}$$

This can be put in matrix form

$$\mathbf{G}q = a, \tag{37}$$

where $\mathbf{G}$ is a $2M + 1$ by $(2N + 1)L$ matrix and q is a $(2N + 1)L$ by one vector of weights.

The solution is then

$$q = \mathbf{G}^H [\mathbf{G}\mathbf{G}^H + \delta \mathbf{I}]^{-1} a, \tag{38}$$

where δ is set to $\varepsilon = 1e - 4$ times the maximum squared singular value of $\mathbf{G}$. Since the array of line sources has the same number of equivalent sources, the spatial Nyquist frequency of the array will be the same as Eq. (34).

C. Simulations

The desired sound field is that produced by a monopole source with sound field coefficients

$$A_m(k) = H_m(kr_s)e^{-im\phi_s}. \tag{39}$$

$L = 15$ higher order sources are used, each of radius $R = 0.25$ m, as in Ref. 1. The activation frequencies for orders 1, 2, and 3 are 216, 433, and 649 Hz, respectively. Simulations are carried out for the second order case, $N = 2$, for which the spatial Nyquist frequency, with $\beta = 0.75$, is 367 Hz.

Sound reproduction is possible over a region r_{max} is possible if the number of loudspeaker sources exceeds the number of modes that are active within that region. From Eq. (29), the radius of accurate reproduction is then[1]

$$r_{max}(f) = \frac{c(\psi L(N + 1/2) - 1/2)}{e \pi f}. \tag{40}$$

The error in the reproduced field is defined here as

$$\varepsilon(r, \phi, k) = \frac{|\hat{p}_I(r, \phi, k) - p_I(r, \phi, k)|}{|p_I(0, k)|}, \tag{41}$$

where $\hat{p}_I(r, \phi, k)$ is the sound field produced by the (higher-order or line-array) loudspeaker array and $p_I(0, k)$ is the sound pressure due to the desired monopole source at the origin. The error was approximately constant within r_{max} and so the accuracy will be quantified by the error within r_{max} in dB.

The first simulation is for reproduction at 250 Hz, well below the spatial Nyquist frequency. This frequency is also below the activation frequency of the second order modes (433 Hz). The array geometries are shown in Fig. 5. Because the source frequency is below the second order activation frequency, the second order source locations are outside the speaker radius, and the second order mode response is about -7 dB in Fig. 3. The effective radius of the line array from Eq. (14) is $y_2 = 2/k = 0.43$ m and so the width is 0.86 m,
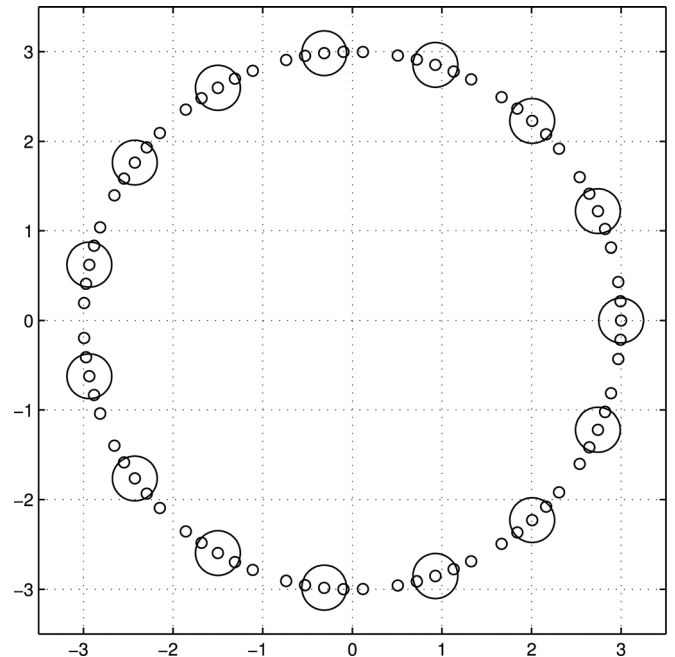

FIG. 5. Higher order and line arrays for 250 Hz and $N = 2$.

although the 7 dB reduction may result in slightly lower performance than an actual line array of monopoles because the loudspeaker weight solutions must compensate for this reduction.

The line array and higher order fields are shown in Figs. 6 and 7 for a source radius of 5 m and a worst-case source angle of 12°, halfway between speakers. The higher order array mode matrix **H** has a condition number of 49.6 and the line array matrix **G** condition number is 20.3. The maximum radius of reproduction from Eq. (40) is 4.4 m which exceeds the loudspeaker radius and so the field is accurate for all regions inside the loudspeaker array. The line array produces an error of around −30 dB and the higher order speakers produce approximately −15 dB. This reduction in accuracy is due to the higher condition number of the matrix **H**, which is probably due to the equivalent monopole sources of the second order phase modes lying outside the speaker radius, with a lower excitation magnitude.

The line arrays produce a continuous locus of wave fronts which is similar to those produced by a regular array of monopoles (see, for example, Figs. 2 and 5 in Ref. 21). The array approximates a single layer potential whose exterior field is equivalently produced by the scattering of the desired field from a pressure release surface at the boundary.[22]

The higher order array produces a lower exterior field for angles near the source angle. This occurs because, as explained above, the higher order apparent source positions are reversed for exterior points. In Fig. 7 the far-field polar response of each higher order source is superimposed on each source, and the two higher-order sources closest to the desired source angle demonstrate a cardioid-like radiation pattern, confirming that the exterior radiation is lower than the interior.

The second simulation is for a source frequency of 800 Hz, which is above the second order activation frequency (433 Hz), but is also well above the spatial Nyquist
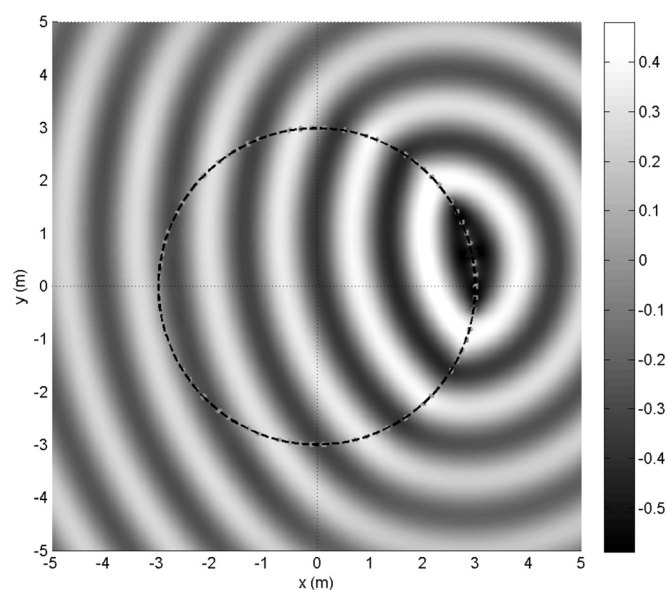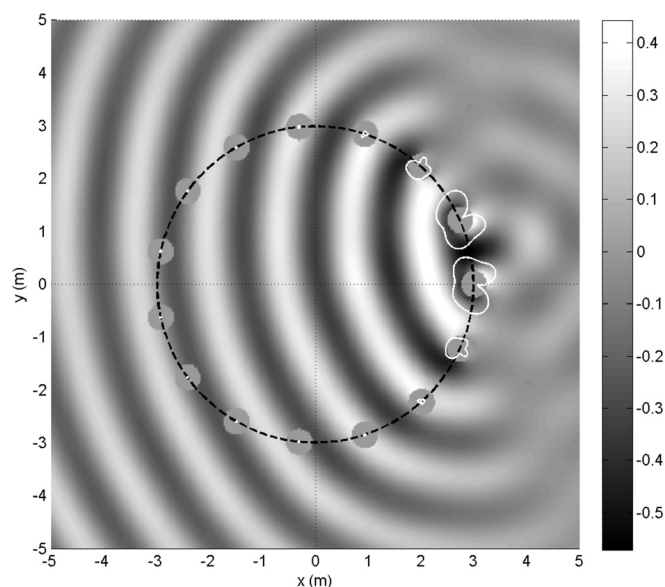

FIG. 7. Higher order sound field for a frequency of 250 Hz and $N = 2$.

frequency (367 Hz). The array geometries are shown in Fig. 8. The line array sources are at radii of 0.068 and 0.135 m and are now well within the radius of the higher order sources.

The reproduced fields are shown in Figs. 9 and 10. The maximum radius from Eq. (40) is 1.37 m, shown as a dashed line in Figs. 9 and 10. This appears to be slightly conservative as the wave field is accurate out to about 1.6 m. The condition numbers of **H** and **G** are 101 and 115, respectively, which are closer to each other than for the 250 Hz simulations. Both solutions are less robust than for the 250 Hz case and the line array and higher order arrays are unable to control the sound field through the entire region inside the arrays. The mean error for radii less than 1.4 m is around −10 dB for both plots.
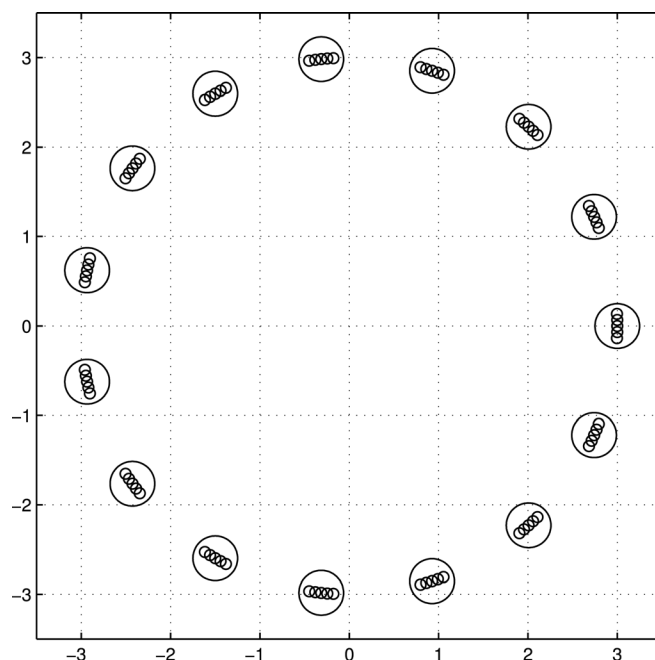

FIG. 6. Line array sound field for a frequency of 250 Hz and five sources per array.

FIG. 8. Higher order and line arrays for 800 Hz and $N = 2$.

Poletti *et al.*: Higher order loudspeaker and line array
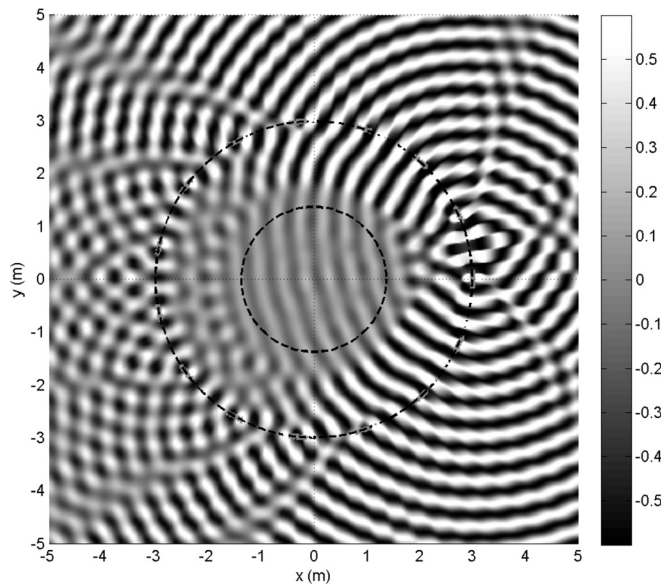
FIG. 9. Line array sound field for a frequency of 800 Hz and five sources per array.

FIG. 11. Sound field for a regular array of $L(2N+1)=75$ monopoles at a frequency of 800 Hz.

The two reproduced fields within the arrays are remarkably similar, showing that the monopole array is equivalent to the higher order source for interior sound field reproduction. There are, however, differences between the interior fields for radii close to the loud-speaker radius r_L, where the higher order apparent source positions start to differ significantly from the assumed line array source positions.

The exterior wave fields are more similar than in the previous case, since both arrays are producing spatial aliasing effects, but the higher order array amplitudes are slightly greater, and the interference is more complicated for angles close to the source angle. Generally, the exterior field with the higher order sources tends to demonstrate greater
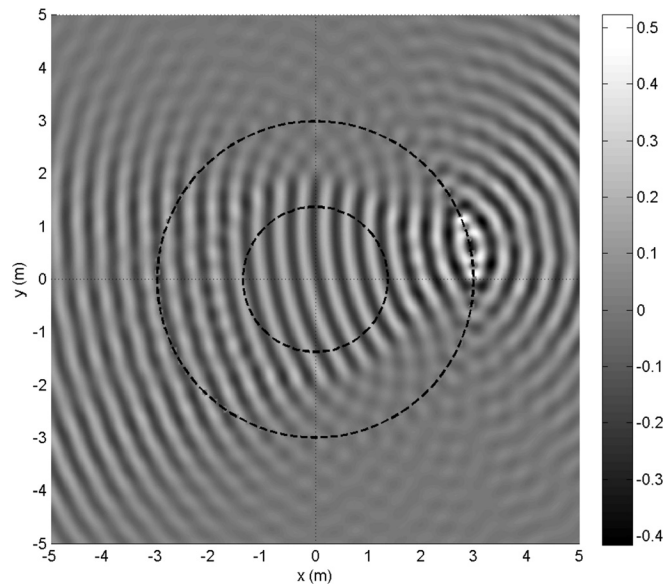
fluctuations, and this is believed to be due to the fact that the source positions are reversed for exterior field positions, and so while the sum of these sources produces the desired field near the origin, the larger phase differences with distance above the spatial Nyquist frequency produce greater fluctuations outside the array.

Finally the sound field produced at 800 Hz by an array of $L(2N+1)=75$ equally spaced monopoles is shown in Fig. 11, to allow comparison with the equivalent higher order source array in Fig. 9. The mode matrix **G** has a reduced condition number of 1.1 and the sound field demonstrates correspondingly less interference, and while the area of accurate reconstruction is similar to that of Fig. 9, the accuracy of reconstruction is better, with a mean error below -40 dB.
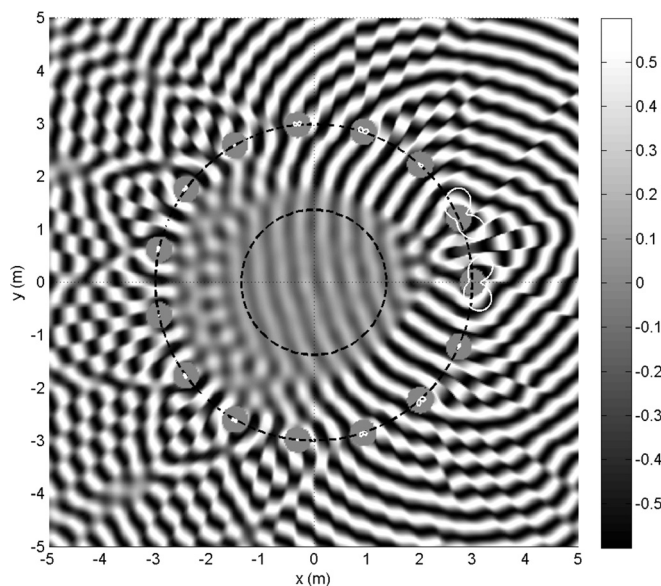
IV. CONCLUSIONS

This paper has shown that a higher order loudspeaker produces phase modes with lines of constant phase that approach an Archimedes spiral. As a result, each mode appears to originate from a different source position, and hence an Nth order source can be viewed as $2N+1$ monopole sources, where the source positions depend on the wavelength, the phase mode order and the field position. Hence, while a higher order source has a physical radius R, it behaves in practice as if it had an aperture governed by the highest order it can radiate at a given frequency, which is frequency dependent. In practice the effective aperture tends to oscillate about $2R$ since the aperture width of the equivalent monopole sources at a given order reduces with frequency, but at higher frequencies higher orders can be radiated to increase the aperture back to $2R$.

Simulations have shown that an array of sources, each of which consists of a line array with sources that match the apparent phase mode source positions, produces an interior field very similar to the higher order source field. However,

FIG. 10. Higher order array sound field for a frequency of 800 Hz and $N=2$.

J. Acoust. Soc. Am., Vol. 136, No. 1, July 2014

Poletti *et al.*: Higher order loudspeaker and line array   199

since the higher order source positions vary with field position, the field close to the loudspeakers, and the exterior sound fields, differ. For frequencies below the spatial Nyquist frequency, the higher order sources tend to produce a lower exterior sound field "upstream" of the direction of propagation, i.e. for angles near the source angle. However, above the spatial Nyquist frequency the higher order array can produce larger amplitudes because the equivalent source positions reverse for exterior field points.

For the reproduction of interior sound fields in free-field conditions, where the room is acoustically treated to reduce wall reflections, a set of L rectangular loudspeakers, each of which is frontally mounted with a single woofer and a line array of $2N+1$ tweeters will produce similar performance to L higher order sources constructed using a circular array of (typically more than $2N+1$) drivers. Such line array devices have been developed for commercial application using wave field synthesis. The results presented here suggest that a regular array of monopole speakers will outperform a higher order array or a non-regular array of monopoles with the same number of sources. However, such arrays require a large number of loudspeaker units which is often impractical.

Higher order sources are able to create equivalent source positions that lie slightly outside the speaker radius, at a reduced but still useful amplitude. The solutions in such cases are not as well-conditioned, but it is thought that the outer sources make some useful contribution to the reproduced field.

The line array equivalent source model gives some insight into the derivation of the spatial Nyquist frequency. If the higher order equivalent sources formed a regular array, the spatial Nyquist frequency would be well-defined and equal to $2N+1$ times the monopole case. However, the equivalent source positions of the higher-order sources reduce with increasing frequency and it is difficult to accurately determine the Nyquist frequency. The result in Eq. (32) gives an approximate value derived from a consideration of the modal dimensionality of the sound field, and which requires an empirical factor $\beta < 1$. Currently no better derivation is known to the authors.

While the equivalent source position radii reduce as the frequency rises, the radii relative to the wavelength are constant. This gives an alternative interpretation of the fact that higher order sources can generate frequency-independent polar responses.

Finally, for sound reproduction in reverberant rooms using calibration and reverberation-cancellation, higher order speakers offer advantages over loudspeaker units containing a line array, because they can rotate the radiated response to any angle.

[1]M. A. Poletti, T. D. Abhayapala, and P. N. Samarasinghe, "Interior and exterior sound field control using two dimensional higher-order variable-directivity sources," J. Acoust. Soc. Am. **131**(5), 3814–3823 (2012).

[2]M. A. Poletti and T. D. Abhayapala, in *Proceedings of the International Conference on Acoustics, Speech and Signal Processing, ICASSP2011*, Prague (2011).

[3]L. Josefsson and P. Persson, *Conformal Array Antenna Theory and Design* (IEEE Wiley, New York, 2006), Chap. 2, pp. 15–46.

[4]G. Ziehm, "Optimum directional pattern synthesis of circular arrays," Radio Electron. Eng. **28**(5), 341–355 (1964).

[5]T. Betlehem, C. Anderson, and M. A. Poletti, in *Proceedings of the 20th International Congress on Acoustics, ICA2010* (2010).

[6]M. A. Poletti, T. Betlehem, and T. D. Abhayapala, in *AES 133rd Convention*, San Francisco (2012).

[7]B. T. Hefner and P. L. Marston, "An acoustic helicoidal wave transducer with applications for the alignment of ultrasonic and underwater systems," J. Acoust. Soc. Am. **106**(6), 3313–3316 (1999).

[8]D. A. Brown, B. Aronov, and C. Bachand, "Cylindrical transducer for producing an acoustic spiral wave for underwater navigation," J. Acoust. Soc. Am. **132**(6), 3611–3613 (2012).

[9]B. T. Hefner and B. R. Dzikowicz, "A spiral wave front beacon for underwater navigation: Basic concept and modeling," J. Acoust. Soc. Am. **129**(6), 3630–3639 (2011).

[10]E. G. Williams, *Fourier Acoustics* (Academic Press, San Diego, 1999), pp. 115–234.

[11]G. N. Watson, *A Treatise on the Theory of Bessel Functions*, 2nd ed. (Cambridge University Press, New York, 1995), Chap. 7, p. 198.

[12]T. L. Heath, *The Works of Archimedes, Edited in Modern Notation with Introductory Chapters* (Cambridge University Press, Cambridge, UK, 1897), pp. 151–188.

[13]D. Colton and R. Kress, *Inverse Acoustic and Electromagnetic Scattering Theory* (Springer, Berlin, 1998), Chap. 2, pp. 13–37.

[14]P. Kassakian and D. Wessel, in *AES 117th Convention*, San Francisco (2004).

[15]M. Pollow and G. K. Behler, "Variable directivity for platonic sound sources based on spherical harmonics optimization," Acta Acust. Acust. **95**(6), 1082–1092 (2009).

[16]B. Rafaely, "Spherical loudspeaker array for local active control of sound," J. Acoust. Soc. Am. **125**(5), 3006–3017 (2009).

[17]A. M. Pasqual, J. R. De França Arruda, and P. Herzog, "Application of acoustic radiation modes in the directivity control by a spherical loudspeaker array," Acta Acust. Acust. **96**(1), 32–42 (2010).

[18]A. M. Pasqual, P. Herzog, and J. R. De França Arruda, "Theoretical and experimental analysis of the electromechanical behaviour of a compact spherical loudspeaker array for directivity control," J. Acoust. Soc. Am. **128**(6), 3478–3488 (2010).

[19]R. Kennedy, P. Sadeghi, T. D. Abhayapala, and H. Jones, "Intrinsic limits of dimensionality and richness in random multipath fields," IEEE Trans. Signal Proc. **55**(6), 2542–2556 (2007).

[20]D. B. Ward and T. D. Abhayapala, "Reproduction of a plane-wave sound field using an array of loudspeakers," IEEE Trans. Speech Audio Process. **9**(6), 697–707 (2001).

[21]J. Ahrens and S. Spors, "An analytical approach to sound field reproduction using circular and spherical loudspeaker distributions," Acta Acust. Acust. **94**, 988–999 (2008).

[22]F. M. Fazi and P. A. Nelson, "Sound field reproduction as an equivalent acoustic scattering problem," J. Acoust. Soc. Am. **134**(5), 3721–3729 (2013).